

Powder-Pattern-Fitting Methods in Structure Determination*

Biserka Gržeta^a and Hideo Toraya^b

^a*Ruder Bošković Institute, P. O. B. 1016, 41001 Zagreb, Croatia*

^b*Ceramics Research Laboratory, Nagoya Institute of Technology, Asahigaoka, Tajimi 507, Japan*

Received February 7, 1994

The Rietveld method is a well known powder-pattern-fitting method which consists in adjusting the complete theoretical diffraction pattern, calculated on the basis of the model for the sample crystal structure, to the experimental powder diffraction pattern. In the fitting procedure, the structure model is being refined. The Rietveld method also enables determination of some other structural properties of the material, like crystallite size and strains, and the quantitative phase analysis of a multicomponent mixture. Complementary fitting methods to the Rietveld method are the individual profile fitting method and the whole-powder-pattern decomposition method, which do not require structural models. The individual profile fitting method enables decomposition of the overlapping diffraction lines in a small range of the powder pattern, while the whole-powder-pattern decomposition method simultaneously decomposes the whole powder pattern into individual lines and refines the unit-cell parameters of the sample. Although the powder-pattern-fitting methods are not methods for direct structure determination, they are very powerful tools in the course of structure determination when the sample is not available in a single crystal form. Several examples of the application of the described methods in structure determination are presented.

INTRODUCTION

Structure analysis from the powder diffraction data is not straightforward because of the problem of peak overlapping. The problem can be overcome, to a considerable extent, by the use of the powder-pattern-fitting methods. The Rietveld method

* Based upon the general lecture presented at the Second Croatian-Slovenian Crystallographic Meeting, Stubičke Toplice, Croatia, Sept. 30 – Oct. 1, 1993.

is a widely used fitting method. This is the method of crystal structure refinement from powder diffraction data (neutron, laboratory X-ray, synchrotron), in which the whole theoretical diffraction pattern, calculated on the basis of a structural model of the sample, is fitted to the experimental diffraction pattern. The method was first reported in 1966 at the 7th Congress of the International Union of Crystallography¹ and published in 1969.² It was originally developed for neutron diffraction data and performed in structure examination of some uranium compounds. Although the method was not immediately recognized as an important technique in the structural study, it is now widely accepted as the fundamentally significant technique for structural study of crystalline materials not available in a single crystal form. Besides, the Rietveld method and other powder-pattern-fitting methods are valuable whenever a fast analysis is feasible (time-resolved studies, phase-diagram determination, *etc.*) because of the shorter time needed to collect powder-diffraction data compared to the single-crystal one. The original paper on the Rietveld method has been cited over 1200 times so far, which indicates how important the method is and how widely it is used.

Structure refinement by means of the Rietveld method can be employed for the compounds containing quite a large number of atoms in the unit cell, such as Sr_4IrO_6 (66 atoms/u.c.),³ or having quite a complex structure, like zeolite ZSM-23 (MMT).⁴ The Rietveld method also enables determination of some other structural properties of the material, like the coherently diffracting domain (crystallite) size and strains, and the quantitative phase analysis of a multicomponent system.

Complementary fitting methods to the Rietveld method are the individual profile fitting⁵ and the whole-powder-pattern decomposition⁶ methods, which do not require structural models. The individual profile fitting method is applied for decomposition of the overlapping diffraction lines in a small range of the powder pattern, and does not need any knowledge of the structure of the investigated material. It gives information on the integrated intensity, peak maximum position and profile shape of individual diffraction lines. The whole-powder-pattern decomposition method requires approximate unit-cell parameters to start the refinement. The method simultaneously decomposes the whole powder pattern into individual lines and refines the unit-cell parameters of the sample.

The reader can find numerous articles dealing with the Rietveld method or other fitting methods, and a recently published book⁷ on this subject. The aim of this paper is to give a short overview of the principles of the fitting methods, starting with the simplest one, the individual profile fitting method, and finishing with the most complex one, the Rietveld method, in an informative form.

INDIVIDUAL PROFILE FITTING METHOD

The procedure of the individual profile fitting method without reference to a structural model was first proposed by Taupin⁸ for X-ray diffractometer data. Sonneveld and Visser⁹ made a variation of the method for use with a Guinier camera film data, while Huang and Parrish,¹⁰ Parrish *et al.*⁵ and Toraya¹¹ improved the original technique.

In general, the fitting method makes use of the numerically recorded powder diffraction pattern in steps of the Bragg angle.¹⁰ The profile intensity at the i th step of the numerically recorded powder pattern, $y(2\theta_i)_{\text{obs}}$, is used as the observed data,

while the corresponding theoretical intensity, $y(2\theta_i)_{\text{calc}}$, may be calculated, for example as¹¹

$$y(2\theta_i)_{\text{calc}} = B(2\theta_i) + \sum_j I_j P(2\theta_i)_j, \quad (1)$$

where $B(2\theta_i)$ is the background intensity, I_j is the integrated intensity of the j th reflection of the sample, $P(2\theta_i)_j$ is the profile function to model the shape of experimental data function and the summation is taken over the neighbouring reflections giving the contribution at $2\theta_i$.

In the case of a multicomponent mixture, the profile intensity is calculated according to

$$y(2\theta_i)_{\text{calc}} = B(2\theta_i) + \sum_j \sum_k I_{jk} P(2\theta_i)_{jk}, \quad (2)$$

where I_{jk} is the integrated intensity of the j th reflection of the k th component, $P(2\theta_i)_{jk}$ is the analogous profile function, and the summation is taken over the neighbouring reflections of all the present components giving the contribution at $2\theta_i$.

The fitting technique consists in adjusting the calculated diffraction intensity to the experimental one by the method of least squares. In the least squares fitting procedure, the following function is minimized

$$D = \sum_i^N w_i [y(2\theta_i)_{\text{obs}} - y(2\theta_i)_{\text{calc}}]^2, \quad (3)$$

where N is the number of observations and w_i is the weight assigned to the i th observation, which is given in the form $1/y(2\theta_i)_{\text{obs}}$.

The quality of fitting result is described by R indices:¹²

$$R_p = \frac{\sum_i^N |y(2\theta_i)_{\text{obs}} - y(2\theta_i)_{\text{calc}}|}{\sum_i^N y(2\theta_i)_{\text{obs}}}, \quad (4)$$

$$R_{wp} = \left\{ \frac{\sum_i^N w_i [y(2\theta_i)_{\text{obs}} - y(2\theta_i)_{\text{calc}}]^2}{\sum_i^N w_i y(2\theta_i)_{\text{obs}}^2} \right\}^{1/2} \quad (5)$$

The order of magnitude of R_p and R_{wp} is $\sim 10\%$ or less.

A very important problem of the powder diffraction pattern fitting methods is what type of the profile function to perform, since the experimental data function is a convolution of the true data function and the instrumental function. Dozens of profile functions have been tested in the profile fitting methods for both neutron and X-ray diffraction. In the neutron angle-dispersive case the diffraction profile is essentially Gaussian.¹ In the case of tube-generated X-rays, the diffraction profile is more complex because of the $K\alpha_1$ - $K\alpha_2$ doublet, long tails of the peak, and the peak asymmetry in low angle region. For this case, the Pearson VII function¹³ and the pseudo-Voigt¹⁴ function showed a better fitting performance. The Pearson VII function is a generalized form of the Lorentzian type function, while the pseudo-Voigt function is the sum of Lorentzian and Gaussian functions in certain proportions. Asymmetry of the experimental data function can be accommodated in several ways. The first is to asymmetrize the symmetric profile function by multiplying it by the following factor²

$$\frac{1 - s(2\theta - T)^2 P}{\tan T} \quad (6)$$

where P is the adjustable parameter and $s = -1$ for $2\theta \leq T$, $s = 1$ for $2\theta > T$. The second way is to dispose the symmetric function asymmetrically.⁵ The third way is to use the split-type profile function, which consists of two parts with different widths and shapes but with the same height at the peak maximum.^{11,15} Generally, the constructed profile function is normalized to have a unit area.

As an example of the individual profile fitting method, the performance of computer program PRO-FIT¹¹ will be described. The profile function to model the diffracted intensity can be selected to be either the split-type Pearson VII or the split-type pseudo-Voigt. The split-type Pearson VII function has the form¹¹

$$P(2\theta)_{\text{PVII}} = \frac{Q}{W} \left[1 + \left(\frac{1+A}{A} \right)^2 (2^{1/R_l} - 1) \left(\frac{2\theta - T}{W} \right)^2 \right]^{-R_l}, \quad \text{for } 2\theta \leq T,$$

$$P(2\theta)_{\text{PVII}} = \frac{Q}{W} \left[1 + (1+A)^2 (2^{1/R_h} - 1) \left(\frac{2\theta - T}{W} \right)^2 \right]^{-R_h}, \quad \text{for } 2\theta > T,$$

$$Q = \frac{2(1+A)}{\pi^{1/2}} \left[A \frac{\Gamma(R_l-1/2)}{(2^{1/R_l}-1)^{1/2} \Gamma(R_l)} + \frac{\Gamma(R_h-1/2)}{(2^{1/R_h}-1)^{1/2} \Gamma(R_h)} \right]^{-1}, \quad (7)$$

where $\Gamma(R)$ is the gamma function, T the peak maximum position, W the full-width at half-maximum (FWHM), A the asymmetry parameter, R_l and R_h the decay rates in the $2\theta \leq T$ and $2\theta > T$ angle regions, respectively. Here, the asymmetry parameter A is explicitly defined as $A = W_l/W_h$, where W_l and W_h are widths of the profile at the low and high angle sides. The split-type pseudo-Voigt function for $2\theta \leq T$ is given by¹⁶

$$P(2\theta)_{p-v} = \frac{(1+A) \left[\eta_h + (1-\eta_h) \sqrt{\pi \ln 2} \right]}{\eta_l + (1-\eta_l) \sqrt{\pi \ln 2} + A \left[\eta_h + (1-\eta_h) \sqrt{\pi \ln 2} \right]} \times \left\{ \eta_l \frac{2}{\pi W} \left[1 + \left(\frac{1+A}{A} \right)^2 \left(\frac{2\theta - T}{W} \right)^2 \right]^{-1} + (1-\eta_l) \frac{2}{W} \sqrt{\frac{\ln 2}{\pi}} \exp \left[- \left(\frac{1+A}{A} \right)^2 \ln 2 \left(\frac{2\theta - T}{W} \right)^2 \right] \right\}, \quad (8)$$

where η_l and η_h are the so-called η parameters at the low- and high-angle sides, respectively, representing mixing ratios of Lorentzian and Gaussian components; $P(2\theta)_{p-v}$ in the range $2\theta > T$ is obtained by exchanging η_l with η_h , η_h with η_l , and A with $1/A$ in (8). The background intensity is represented by the second order polynomial of 2θ

$$B(2\theta) = b_1 + b_2 2\theta + b_3 (2\theta)^2. \quad (9)$$

Adjustable least-squares parameters in PRO-FIT are listed in Table I. In the fitting procedure, the parameters are varied until function (3) is minimized. The least-squares procedure is terminated when all the parameters converge, *i.e.* their changes become less than 5% of the respective estimated standard deviations (e.s.d.), or when

TABLE I

List of least-squares parameters in PRO-FIT

b_1, b_2, b_3	Background level (counts)
K	Intensity ratio of $K\alpha_1$ to $K\alpha_2$
e	Correction of the difference $\lambda_2 - \lambda_1$ (Å)
I_j	Integrated intensity of the j th peak (counts)
T_j	Peak maximum position (2θ)
W_j	Full-width at half-maximum (FWHM) (2θ)
A_j	Peak asymmetry
$R_{lj}; \eta_{lj}$	Decay rate of profile intensity at the low angle side; or η parameter at the low angle side
$R_{hj}; \eta_{hj}$	Decay rate of profile intensity at the high angle side; or η parameter at the high angle side

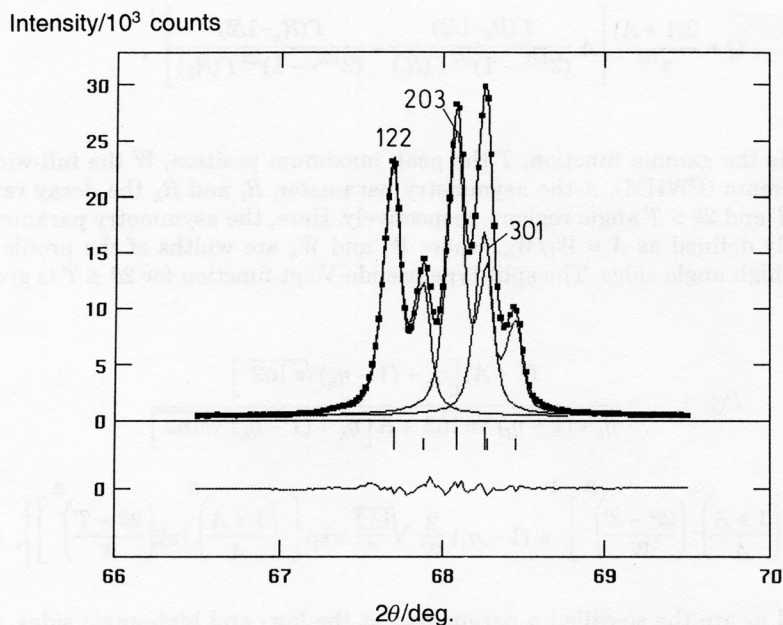


Figure 1. Individual profile fitting result for α -SiO₂ in the selected 2θ range (Cu $K\alpha$ data; the split-type pseudo-Voigt profile model and the polynomial background model in calculations). Observed profile intensity is represented by symbol ■, and the calculated one by the solid line. Differences between the two intensities are plotted at the bottom of the diagram on the same scale as above. Vertical bars are the reflection position markers, longer for Cu $K\alpha_1$ and shorter for Cu $K\alpha_2$ positions. $R_p = 0.023$, $R_{wp} = 0.037$.

the R_{wp} factor (5) does not change in successive three least-squares cycles. Selected individual profile fitting results for α -SiO₂ (with X-rays) and C₁₇H₁₃CuN₃O₄ (with synchrotron radiation)¹⁷ are presented in Figures 1 and 2 and Table II.

TABLE II

Output of the PRO-FIT program giving the refined least-squares parameters for α -SiO₂ in the Bragg angle range $2\theta = 66.5^\circ$ – 69.5° (shown in Figure 1). The e. s. d.'s are given below the corresponding parameters. $R_p = 0.023$, $R_{wp} = 0.037$.

	b_1	b_2	b_3	K	e	
	455.84	0.00	0.00	0.497	0.00	
	8.93	0.00	0.00	0.000	0.00	
Peak	I	T	W	A	η_l	η_h
1	5369.15	67.692955	0.120420	1.529327	0.574032	0.791875
	36.65	0.001227	0.000970	0.070099	0.022578	0.038500
2	6133.98	68.091042	0.120420	1.529327	0.574032	0.791875
	53.05	0.001225	0.000970	0.070099	0.022578	0.038500
3	3894.94	68.264832	0.120420	1.529327	0.574032	0.791875
	49.63	0.001326	0.000970	0.070099	0.022578	0.038500

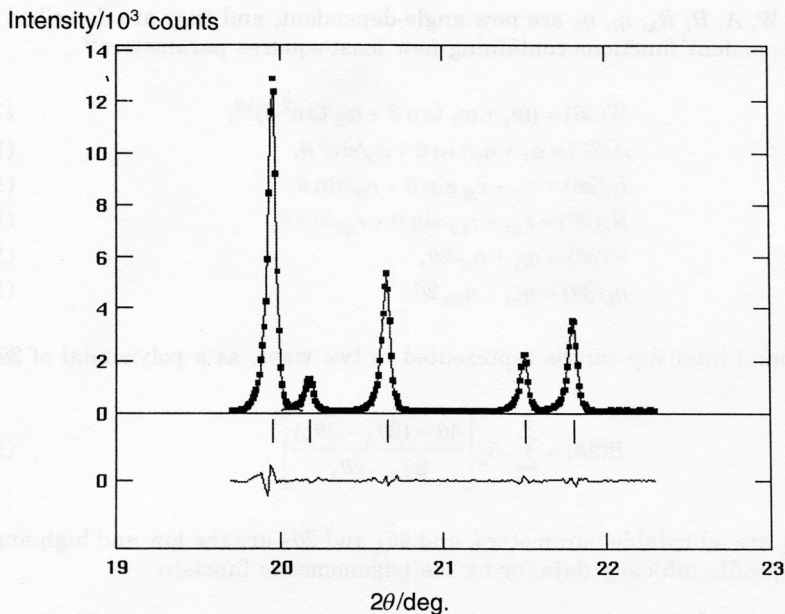


Figure 2. Individual profile fitting result for $C_{17}H_{13}CuN_3O_4$ (Ref. 17; synchrotron data with $\lambda = 1.53286 \text{ \AA}$, the split-type Pearson VII profile model and the polynomial background model in calculations). The diagrams are shown as in Figure 1. Upper short vertical bars represent the Bragg reflection positions. $R_p = 0.053$, $R_{wp} = 0.077$.

WHOLE-POWDER-PATTERN DECOMPOSITION METHOD

The whole-powder-pattern decomposition method (WPPD) decomposes the whole powder pattern into individual reflections and refines the unit-cell parameters in one step. The method was first introduced by Pawley⁶ as the method for analyzing the neutron powder diffraction data, while Toraya¹¹ proposed a method for analyzing X-ray diffraction data. The WPPD method is not as common as the Rietveld method, but it is of great importance for the powder data analysis, in particular in the field of materials science.¹⁸

The method requires approximate unit-cell parameters to start the fitting. The initial unit-cell parameters make it possible to calculate positions of possible diffraction lines in the whole region of the Bragg angles. If the unit cell is nearly correct, the diffraction peak positions are calculated nearby, and should approach the observed peaks by the change (refinement) of the unit-cell parameters in the fitting procedure.⁶

Here, the principles of the WPPF (whole-powder-pattern fitting) computer program^{11,18} will be described. The program adopts two profile functions, the split-type Pearson VII function and the split-type pseudo-Voigt function, defined by (7) and (8). The peak maximum position T_j is the function of unit cell parameters. It can be corrected for the peak shift arising from the zero-point shift and the peak asymmetry by

$$T(2\theta) = t_1 + t_2 \tan\theta + t_3 \tan^2\theta. \quad (10)$$

Parameters W , A , R_l , R_h , η_l , η_h are now angle-dependent, and they are described by the angle-dependent functions containing new least-squares parameters¹¹

$$W(2\theta) = (w_1 + w_2 \tan \theta + w_3 \tan^2 \theta)^{1/2}, \quad (11)$$

$$A(2\theta) = a_1 + a_2/\sin \theta + a_3/\sin^2 \theta, \quad (12)$$

$$R_l(2\theta) = r_{l1} + r_{l2} \sin \theta + r_{l3}/\sin \theta, \quad (13)$$

$$R_h(2\theta) = r_{h1} + r_{h2} \sin \theta + r_{h3}/\sin \theta, \quad (14)$$

$$\eta_l(2\theta) = \eta_{l1} + \eta_{l2} 2\theta, \quad (15)$$

$$\eta_h(2\theta) = \eta_{h1} + \eta_{h2} 2\theta. \quad (16)$$

The background intensity can be represented in two ways, as a polynomial of 2θ

$$B(2\theta) = \sum_{k=1}^6 b_k \left[\frac{4\theta - (2\theta_A - 2\theta_B)}{2\theta_B - 2\theta_A} \right]^k, \quad (17)$$

where $b_1 \dots b_6$ are adjustable parameters, and $2\theta_A$ and $2\theta_B$ are the low and high angle 2θ limits of profile intensity data, or by the trigonometric function

$$B(2\theta) = b_1 + b_2 2\theta + b_3 \sin \theta + b_4 \tan \theta, \quad (18)$$

where $b_1 \dots b_4$ are adjustable parameters. The powder diffraction data of a multicomponent mixture can also be analyzed by WPPF. The profile function is then calculated according to (2) by taking into account the global parameters (common to all components) and parameters for each component. Adjustable least-squares parameters in WPPF are listed in Table III. The flow of the least-squares fitting procedure

TABLE III

List of least-squares parameters in WPPF

Global parameters	
$b_1, b_2, b_3, b_4, b_5, b_6$	Background level
K	Intensity ratio of $K\alpha_1$ to $K\alpha_2$
e	Correction of the difference $\lambda_2 - \lambda_1$ (Å)
t_1, t_2, t_3	Peak shift correction (2θ)
Parameters for each component	
I_j	Integrated intensity of the j th peak (counts)
$a, b, c, \alpha, \beta, \gamma$	Unit-cell parameters
w_1, w_2, w_3	Full width at half-maximum (FWHM) (2θ)
a_1, a_2, a_3	Peak asymmetry
r_{l1}, r_{l2}, r_{l3}	Decay rate of profile intensity at the low angle side;
η_{l1}, η_{l2}	or η parameter at the low angle side
r_{h1}, r_{h2}, r_{h3}	Decay rate of profile intensity at the high angle side;
η_{h1}, η_{h2}	or η parameter at the high angle side

is the same as in the case of the individual profile fitting, *i.e.* the least-squares parameters are varied until the function (3) is minimized.

If the sample contains an internal standard reference material, its unit-cell parameters should be kept fixed in the least-squares procedure. In this way the peak-shift parameters (t_1, t_2, t_3) and the unit-cell parameters of the investigated sample/component are best refined.

The result of WPPF are refined least-squares parameters, including refined unit-cell parameters of the sample, the reflections list ($hkl, d, I/I_1$ values) and a graphical presentation of the observed and calculated powder patterns.

As an example, the whole-powder-pattern decomposition of the sample $\text{Sr}_2\text{SmTaCu}_2\text{O}_8$ ¹⁹ will be described. The fitting was performed in the range $2\theta = 10^\circ - 100^\circ$ by the WPPF program. Silicon was added into the sample as the internal standard. The refinement started by varying the background and integrated intensities, and the number of varied parameters was gradually increased in successive fitting cycles. After 13 cycles, the least-squares parameters converged to

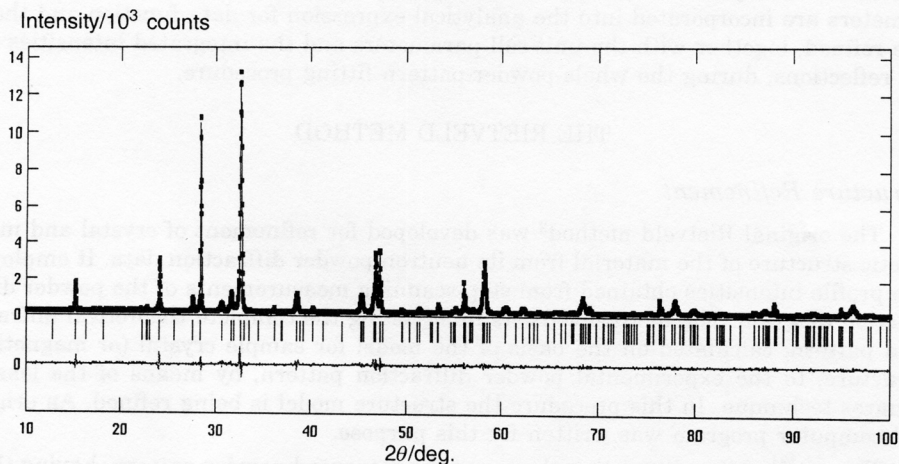


Figure 3. Whole-powder-pattern decomposition result for $\text{Sr}_2\text{SmTaCu}_2\text{O}_8$ (Ref. 19) with Si as internal standard (Cu $K\alpha$ data; the split-type pseudo-Voigt profile model and the polynomial background model in calculations). The diagrams are shown as in Figure 1. Upper short vertical bars represent the Bragg reflection positions of the sample. $R_p = 0.065$, $R_{wp} = 0.085$.

$R_{wp} = 0.117$, but some low-intensity lines remained unidentified. By introducing the unit-cell parameters for $\text{Sr}(\text{Cu}_{0.33}\text{Ta}_{0.67})\text{O}_3$ as an impurity component, the R_{wp} decreased to 0.085 in 9 cycles. Figure 3 shows the observed and calculated powder patterns of the examined sample, while the unit-cell parameters and other refined least-squares parameters of $\text{Sr}_2\text{SmTaCu}_2\text{O}_8$ are listed in the Table IV.

The whole-powder-pattern decomposition method is also applicable for determination of coherently diffracting domain size and strains.^{20,21} The computer program TOMOE²¹ can be employed for this purpose. The fitting function used is defined as the sum of the background intensity and contributions from individual reflections,

TABLE IV

Refined WPPF least-squares parameters for $Sr_2SmTaCu_2O_8$ (tetragonal, $S.G. = P4/mmm$)¹⁹

$b_1 = 218$ (1)	$b_2 = 43$ (4)	$b_3 = -8$ (7)
$b_4 = -212$ (17)	$b_5 = 28$ (8)	$b_6 = 180$ (15)
$K = 0.497$	$e = 0$	
$t_1 = -0.002$ (1)	$t_2 = 0.023$ (5)	$t_3 = -0.019$ (5)
$a = 3.8741$ (2) Å	$c = 11.6654$ (8) Å	
$w_1 = 0.005$ (1)	$w_2 = 0.014$ (7)	$w_3 = 0.089$ (10)
$a_1 = 0.904$ (24)	$a_2 = 0$	$a_3 = 0$
$\eta_{l1} = 0.955$ (25)	$\eta_{l2} = 0$	
$\eta_{h1} = 0.516$ (23)	$\eta_{h2} = 0$	
$R_p = 0.065$	$R_{wp} = 0.085$	

given as the convolution of the observed instrumental function with the true data function in analytical form. The coherently diffracting domain size and strain parameters are incorporated into the analytical expression for data function and they are refined, together with the unit-cell parameters and the integrated intensities of all reflections, during the whole-powder-pattern fitting procedure.

THE RIETVELD METHOD

Structure Refinement

The original Rietveld method² was developed for refinement of crystal and magnetic structure of the material from its neutron powder diffraction data. It employs the profile intensities obtained from step-scanning measurements of the powder diffraction diagram. The method consists in adjusting the complete theoretical diffraction pattern, calculated on the basis of the model for sample crystal (or magnetic) structure, to the experimental powder diffraction pattern, by means of the least-squares technique. In this procedure the structure model is being refined. An original computer program was written for this purpose.

The profile intensity at the i th step of the measured powder pattern, having the background subtracted, is used as the observed data. The corresponding theoretical contribution can be calculated according to²

$$y(2\theta_i)_{\text{calc}} = \sum_k w_{i,k} S_k^2, \quad (19)$$

where $w_{i,k}$ is a measure of the contribution of the diffraction peak with the maximum at position $2\theta_k$ to the diffraction profile at position $2\theta_i$. It is a function of the counter step width, the halfwidths of the diffraction peaks, the Lorentz factor, profile asymmetry and the multiplicity of the reflections. S_k is a structure factor containing nuclear and magnetic contributions, $S_k^2 = F_k^2 + J_k^2$. The summation is taken over the neighbouring peaks which give the contribution at $2\theta_i$. The Gaussian peak shape is assumed for each Bragg peak, accommodated for asymmetry by (6). In the least-squares refinement, the following function is minimized with respect to the least-squares parameters

$$M = \sum_i^N w_i \left[y(2\theta_i)_{\text{obs}} - \frac{1}{c} y(2\theta_i)_{\text{calc}} \right]^2, \quad (20)$$

where N is the number of independent observations, w_i is a weight assigned to the i th observation, and c is the overall scale factor. The least-squares parameters are divided into two groups: profile parameters and structure parameters, as listed in Table V. Structure parameters correspond to the asymmetric unit. In order to describe the content of the complete unit cell, the set of symmetry operations should also be given as input data for the program. The quality of the fitting result is described by the following R indices: R_{total} , R_{nuclear} , R_{magnetic} and R_{profile} . Definitions can be found in the original paper.²

TABLE V

List of least-squares parameters in the original Rietveld refinement

Profile parameters	
U, V, W	Halfwidth parameters
Z	Counter zero point
A, B, C, D, E, F	Unit-cell parameters
P	Asymmetry parameter
G	Preferred orientation parameter
Structure parameters	
c	Overall scale factor, such that $Y_{\text{calc}} = c Y_{\text{obs}}$
Q	Overall isotropic temperature parameter
x_i, y_i, z_i	Fractional coordinates of the i th atom in the asymmetric unit
B_i	Atomic isotropic temperature parameter
n_i	Site occupation number
$K_{x,i}, K_{y,i}, K_{z,i}$	Components of the magnetic vector of the i th atom in the asymmetric unit

The Rietveld refinement method developed for neutron powder diffraction data has been extended for the use with X-ray diffraction data. Malmros and Thomas²² varied the original Rietveld program for the use with powder X-ray film data applying a modified Lorentz profile function instead of Gaussian. Young, Mackie and Von Dreele²³ adopted the Rietveld method to be applicable for the X-ray powder diffractometer data by including atomic scattering factors, Lorentz and polarization factors, absorption correction and the alpha doublet.

As the interest for the Rietveld refinement increased, new versions of programs appeared,²⁴ most of them prepared to be used with a multicomponent powder sample. This improved the applicability of the Rietveld method to the neutron as well as to X-ray and synchrotron diffraction data, not only in structure refinement but also in determination of the coherently diffracting domain size and strains and quantitative phase analysis. Nowadays, the most widely used programs are the DBWS,²⁵ GSAS²⁶ and RIETAN²⁷ programs.

As an example, the structure refinement of α -SiO₂ will be presented, performed by the X-ray powder diffractometer data and the pattern-fitting program PFLS written by Toraya and Marumo.²⁸ The least-squares parameters in the PFLS program included profile and structure parameters. The profile function could be selected to be either the split-type pseudo-Voigt or the split-type Pearson VII. The refinement quality is described by the R indices defined by (4) and (5). Fitting procedure was performed for the Bragg angles range $2\theta = 30^\circ - 140^\circ$, using the split-type pseudo-Voigt profile function and the polynomial background model (17). After 12 cycles, parameters converged to $R_{wp} = 0.069$. The observed and calculated powder patterns of α -SiO₂ are presented in Figure 4, while the refined structural parameters of α -SiO₂ are listed in Table VI.

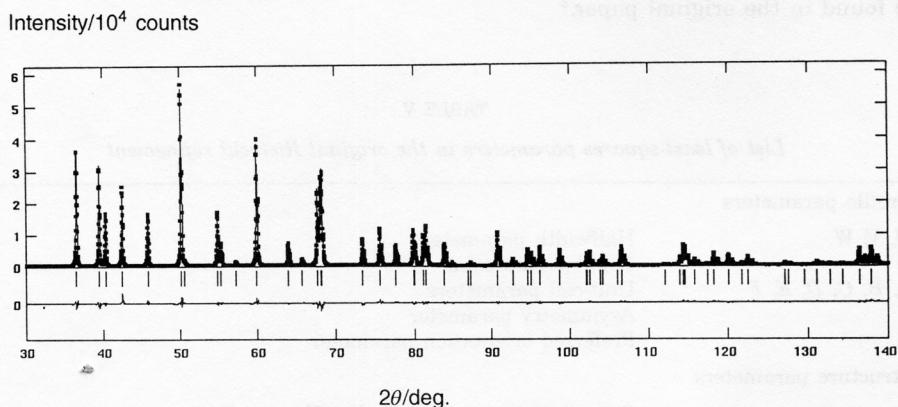


Figure 4. Result of the Rietveld refinement for α -SiO₂ (Cu $K\alpha$ data; the split-type pseudo-Voigt profile model and the polynomial background model in calculations). The diagrams are shown as in Figure 1. Upper short vertical bars represent the Bragg reflection positions. $R_p = 0.052$, $R_{wp} = 0.069$.

TABLE VI

Refined structural parameters of α -SiO₂ (S.G. = P3₁21, $a = 4.9127$, $c = 5.4042$ Å) obtained by the PFLS program (the e.s.d.'s are given below the corresponding parameters). $R_p = 0.052$, $R_{wp} = 0.069$.

Atom	Site	Site occupation	x	y	z	$B_{iso} / \text{Å}^2$
Si	3b	0.50	0.470608	0.000000	0.166667	0.4086
		0.00	0.000098	0.000000	0.000000	0.0081
O	6c	1.00	0.414604	0.268247	0.287255	0.8693
		0.00	0.000158	0.000160	0.000122	0.0185

Quantitative Phase Analysis Using the Rietveld Method

The fact that the Rietveld method is applicable to the multicomponent sample has increased interest in finding out how to use the method in the quantitative phase analysis.

Werner *et al.*²⁹ were the first to report the quantitative phase analysis using the Rietveld method. They made use of the Guinier-Hägg X-ray powder film data. Toraya *et al.*³⁰ applied the method to X-ray powder diffractometer data, while Hill and Howard³¹ proposed a variation of the method to be used with the neutron powder diffractometer data. These methods for quantitative phase analysis need no previously determined calibration curve and make use of the whole powder diffraction data. According to Hill and Howard,³¹ the weight fraction W of the phase p is given by

$$W_p = \frac{S_p (ZMV)_p}{\sum_i S_i (ZMV)_i}, \quad (21)$$

where S , Z , M and V are the scale factor determined in the Rietveld refinement, the number of formula units per unit cell, the mass of the formula unit and the unit-cell volume of the component, respectively. Summation is performed over all the components in the system.

Although several other methods have been reported later, the methods mentioned above are mostly used with the Rietveld refinement data.

COMPARISON OF THE POWDER-PATTERN-FITTING METHODS

The individual profile fitting method, the whole-powder-pattern decomposition (WPPD) method and the Rietveld method are compared in Table VII.¹⁸ The properties of the method indicate their place and role in the structure analysis of the powder material. A possible sequence of using the methods is given in Figure 5. This is, in fact, the path of the *ab initio* structure determination.

TABLE VII
Comparison of the powder-pattern-fitting methods

	Individual profile fitting	Whole-powder-pattern-decomposition (WPPD) method	Rietveld method
Aim of analysis	Pattern decomposition	Pattern decomposition and refinement of unit-cell parameters	Structure refinement
Range of analysis	Local pattern	Whole pattern	Whole pattern
Profile model	Peak position	Function of unit-cell parameters	Function of unit-cell parameters
	Profile area (integrated intensity)	Independent parameters	Function of structural parameters
	Profile shape	Angle-independent	Angle-dependent
Initial parameters required to start the refinement	Null	Approximate unit-cell parameters	Initial structural parameters

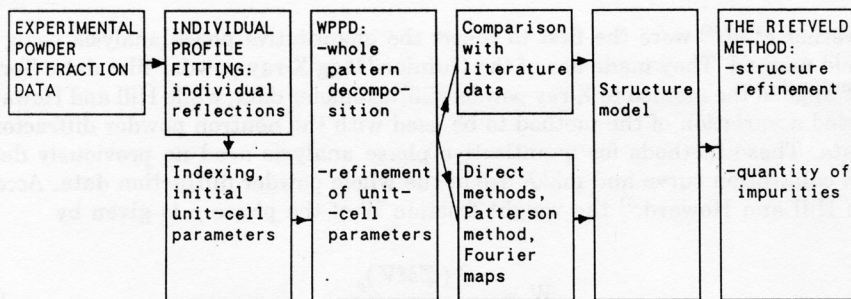


Figure 5. A possible sequence of using the powder-pattern-fitting methods in structure determination from the powder sample.

Each of the described powder fitting methods can be used independently of the others, but they are complementary in terms of their results. They have one important property in common: all of them can be applied to the multicomponent powder sample.

PRECISION AND ACCURACY OF THE POWDER-PATTERN-FITTING METHODS

The powder-pattern-fitting methods employ experimental diffraction data and theoretical diffraction data calculated on the basis of analytical expressions for the background and profile functions. Thus, both experimental and theoretical data errors affect the final fitting result.

The main cause of experimental systematic errors are the preferred orientation and bad particle statistics in the powder sample. Main theoretical systematic errors may be caused by the profile and background modelings, and by profile function truncation. Most of the analytical functions used for representing the diffracted profile shape are mathematically defined in the infinitely large interval; however, in the fitting procedure they are calculated in a finite range of Bragg angles, *i.e.* the tails are truncated. The truncation of a profile function induces appreciable errors in the calculated intensities, and thus in the fitting result as well.³² The main strategy for suppressing the truncation error is to extend the definition range of the profile function to include more than 99% of the profile area.³² This is especially important in the case of strong non-Gaussian reflections.

Other systematic errors, mentioned above, may be minimized by a careful preparation of the powder sample, by using high-resolution diffraction data and by improving the profile and background modelings.

A very instructive review on the precision and accuracy of the Rietveld method is the report on the Rietveld Refinement Round Robin.³³ In this project of the Commission on Powder Diffraction of the International Union of Crystallography, the structure of the compound PbSO_4 has been refined from two 'standard' PbSO_4 powder diffraction patterns, a conventional X-ray diffraction and a neutron diffraction pattern, by 23 world-wide participants. Eighteen refinements with the X-ray data and twenty refinements with the neutron data have been performed by means of 11 different computer programs. The results in average show a very good agreement of the refined structure with the structure determined from a single crystal.

CONCLUSIONS

Three powder-pattern-fitting methods have been presented: the individual profile fitting, the whole pattern decomposition and the Rietveld method. They are complementary in terms of their results and they represent powerful tools for structure investigations of a polycrystalline sample (single phase or multicomponent). To achieve good precision and accuracy in the performance of the described methods, special attention should be paid to sample preparation, resolution of diffraction data and to the choice of the profile and background models to be used in calculations.

REFERENCES

1. H. M. Rietveld, Abstracts of the 7th Congress and Symposium of the International Union of Crystallography, Moscow 1966, *Acta Cryst.* **21**, Suppl. (1966) A228.
2. H. M. Rietveld, *J. Appl. Cryst.* **2** (1969) 65.
3. A. V. Powell, P. D. Battle, and J. G. Gore, *Acta Cryst.* **C49** (1993) 852.
4. B. Marler, C. Deroche, H. Gies, C. A. Fyfe, H. Grondey, G. T. Kokotailo, Y. Feng, S. Ernst, J. Weitkamp, and D. E. Cox, *J. Appl. Cryst.* **26** (1993) 636.
5. W. Parrish, T. C. Huang, and G. L. Ayers, *Trans. Am. Cryst. Assoc.* **12** (1976) 55.
6. G. S. Pawley, *J. Appl. Cryst.* **14** (1981) 357.
7. R. A. Young (Ed.) *The Rietveld Method*, IUCR Monographs on Crystallography **5**, Oxford University Press, Oxford, 1993.
8. D. Taupin, *J. Appl. Cryst.* **6** (1973) 266.
9. E. J. Sonneveld and J. W. Wiesser, *J. Appl. Cryst.* **8** (1975) 1.
10. T. C. Huang and W. Parrish, *Appl. Phys. Letters* **27** (1975) 123.
11. H. Toraya, *J. Appl. Cryst.* **19** (1986) 440.
12. R. A. Young, E. Prince, and R. A. Sparks, *J. Appl. Cryst.* **5** (1982) 357.
13. M. M. Hall, Jr., V. G. Veeraraghavan, H. Rubin, and P. G. Winchell, *J. Appl. Cryst.* **10** (1977) 66.
14. G. K. Wertheim, M. A. Butler, K. W. West, and D. N. E. Buchanan, *Rev. Sci. Instrum.* **45** (1974) 1369.
15. C. G. Windsor and R. N. Sinclair, *Acta Cryst.* **A32** (1976) 395.
16. H. Toraya, *J. Appl. Cryst.* **23** (1990) 485.
17. B. Gržeta, H. Toraya, and M. Herceg, Abstracts of the 2nd Croatian-Slovenian Crystallographic Meeting, Stubičke Toplice, Croatia, 1993, p. 23; to be published elsewhere.
18. H. Toraya, *The Rigaku Journal* **6** (1989) 28.
19. B. Gržeta, H. Toraya, N. Brničević, P. Planinić, and I. Bašić, Abstracts of the 2nd Croatian-Slovenian Crystallographic Meeting, Stubičke Toplice, Croatia, 1993, p. 38, to be published elsewhere.
20. H. Toraya, *J. Appl. Cryst.* **21** (1988) 192.
21. H. Toraya, *Powder Diffraction* **4** (1989) 130.
22. G. Malmros and J. O. Thomas, *J. Appl. Cryst.* **10** (1997) 7.
23. R. A. Young, P. E. Mackie, and R. B. Von Dreele, *J. Appl. Cryst.* **10** (1977) 262.
24. D. K. Smith and S. Gortler, *Powder Diffraction Program Information, Release 2.0*, Powder Diffraction Program Information Centre, Leiden, The Netherlands, 1992.
25. D. B. Wiles and R. A. Young, *J. Appl. Cryst.* **14** (1981) 149.
26. A. C. Larson and R. B. Von Dreele, *GSAS, Generalized Crystal Structure Analysis System*, LAUR-86-748, Los Alamos National Laboratory, Los Alamos, USA, 1987.
27. F. Izumi, *The Rigaku Journal* **6** (1989) 10.
28. H. Toraya and F. Marumo, *Rep. Res. Lab. Eng. Mater. Tokyo Inst. Technol.* **5** (1980) 55.
29. P.-E. Werner, S. Salome, G. Malmros, and J. O. Thomas, *J. Appl. Cryst.* **12** (1979) 107.
30. H. Toraya, M. Yoshimura, and S. Somiya, *J. Am. Ceram. Soc.* **67** (1984) C119.
31. R. J. Hill and C. J. Howard, *J. Appl. Cryst.* **20** (1987) 467.
32. H. Toraya, *J. Appl. Cryst.* **18** (1985) 351.
33. R. J. Hill, *J. Appl. Cryst.* **25** (1992) 589.

SAŽETAK

Metode usklađivanja difrakcijskih slika praha u određivanju kristalne strukture*Biserka Gržeta i Hideo Toraya*

Rietveldova metoda vrlo je poznata metoda koja se sastoji u usklađivanju teorijske difrakcijske slike praha materijala, izračunane na osnovi modela njegove kristalne strukture, s eksperimentalnom difrakcijskom slikom praha. U procesu usklađivanja strukturni se model utočnjava, tj. približava se stvarnoj kristalnoj strukturi. Rietveldova metoda također omogućuje određivanje još nekih kristalnih osobina materijala kao što su veličina kristalita i naprezanja kristalne rešetke, te kvantitativnu faznu analizu višekomponentnog materijala. Metode komplementarne Rietveldovoj metodi jesu metoda usklađivanja pojedinačnih difrakcijskih linija i metoda dekompozicije cijele difrakcijske slike. Te metode ne zahtijevaju početni strukturni model. Metoda usklađivanja pojedinačnih difrakcijskih linija omogućuje razlučivanje pojedinačnih linija u uskomu kutnom području difrakcijske slike praha, dok metoda dekompozicije cijele difrakcijske slike istovremeno razlučuje difrakcijsku sliku na pojedinačne linije u cijelom kutnom području i utočnjava parametre jedinične ćelije uzorka. Premda metode usklađivanja difrakcijskih slika praha nisu metode za direktno određivanje strukture, one su vrlo djelotvorne pri rješavanju strukture kada se materijal ne može prirediti u obliku monokristala. U radu je prikazano nekoliko primjera primjene tih metoda pri određivanju strukture.